

# Solar Blind Photodetectors Enabled by Nanotextured $\beta$ -Ga<sub>2</sub>O<sub>3</sub> Films Grown via Oxidation of GaAs Substrates

Dewyani Patil-Chaudhari<sup>1\*</sup>, Matthew Ombaba<sup>1\*</sup>, Jin Yong Oh<sup>1</sup>, Howard Mao<sup>1</sup>, Kyle H. Montgomery<sup>1</sup>, Andrew Lange<sup>2</sup>, Subhash Mahajan<sup>2</sup>, Jerry M. Woodall<sup>1</sup> and M. Saif Islam<sup>1†</sup>

<sup>1</sup>Department of Electrical and Computer Engineering, University of California, One Shield Avenue, Davis, CA 95616, USA

<sup>2</sup>Department of Materials Science and Engineering, University of California, One Shield Avenue, Davis, CA 95616, USA

<sup>†</sup>Email: sislam@ucdavis.edu

**Abstract**—A simple and inexpensive method for growing Ga<sub>2</sub>O<sub>3</sub> using GaAs wafers was demonstrated. Si-doped GaAs wafers were heated to 1050°C in a horizontal tube furnace in both argon and air ambients in order to convert their surfaces to  $\beta$ -Ga<sub>2</sub>O<sub>3</sub>. The  $\beta$ -Ga<sub>2</sub>O<sub>3</sub> films were characterized using SEM, EDX and X-ray diffraction. They were also used to fabricate solar blind photodetectors. The devices, which had nano-textured surfaces, exhibited a high sensitivity to UV illumination due in part to large surface areas. Furthermore, the films had coherent interfaces with the substrate, which led to a robust device with high resistance to thermomechanical stress. The photoconductance of the  $\beta$ -Ga<sub>2</sub>O<sub>3</sub> films was found to increase by more than three orders of magnitude under 270 nm ultraviolet (UV) illumination with respect to the dark current. The fabricated device showed a responsivity of ~292 mA/W at this wavelength.

**Index Terms**— beta-gallium oxide, gallium arsenide, oxidation, photodetector, solar-blind detector

## I. INTRODUCTION

Solar blind photodetectors are able to respond exclusively to deep UV radiation even in the presence of light from other regions of the electromagnetic spectrum. This makes them suitable for a number of applications for which deep UV detection is necessary or for which solar light pollution is a problem. Applications of such devices include tracking of missile signatures, flame detection, non-line-of-sight optical communication and ozone layer monitoring [1]. Although solar blind detectors have been fabricated using a number of wide band-gap semiconductors such as MgZnO [2] and alloys [3], AlGaIn [4], diamond [5], MgS [6], and ZrTiO<sub>2</sub> [7], they suffer from low sensitivity across the wavelengths of interest, high material complexity, and high fabrication costs.

Some of these challenges can be addressed by using gallium oxide (Ga<sub>2</sub>O<sub>3</sub>), a wide band-gap semiconductor (4.2-4.9 eV) that is both chemically and thermally stable. Ga<sub>2</sub>O<sub>3</sub> photodetectors have been fabricated in the form of thin films [8], nanowires [9], single nano-bridges [10], nano-ridges, nano-sheets [11], nano-rods [12], and micro-porous deposits [13] using a range of deposition techniques including atomic layer deposition [14], electrochemical deposition [15], molecular beam epitaxy [16], pulsed laser deposition [17], sputtering [18], and chemical vapor deposition [19]. A recurring theme with the above approaches is the use of *bottom-up* fabrication techniques to generate Ga<sub>2</sub>O<sub>3</sub> structures. So far, these techniques suffer from reproducibility, high cost, and limited control over morphology and microstructure. Additionally, many of the previously grown Ga<sub>2</sub>O<sub>3</sub> nanostructures lack coherent interfaces with their substrates, which make them prone to separation when exposed to thermal and mechanical stress. Lv et al. [20] observed that deposition of Ga<sub>2</sub>O<sub>3</sub> at high temperatures led to peeling off of the product from the growth substrate due to mismatch between the coefficient of thermal expansion of Ga<sub>2</sub>O<sub>3</sub> and the substrate. While oxidizing GaAs and GaN through wet thermal oxidation, Korbutowicz et al. [21] discovered that with longer oxidation times of around 300 minutes, gallium oxide layers cracked and showed exfoliation. It was argued that the cracks were caused by strain at the GaAs/Ga<sub>2</sub>O<sub>3</sub> interface. Hwang et al. [22] found that  $\beta$ -Ga<sub>2</sub>O<sub>3</sub> membranes could be easily exfoliated from bulk crystals even though they are 3D. This was due to the anisotropic chemical bonds with strong in-plane covalent bonds and much weaker van der Waals bonds. Some researchers have successfully immobilized Ga<sub>2</sub>O<sub>3</sub> nanostructures on top of foreign substrates; however, to fabricate these nanostructures into devices, additional low yield patterning techniques are required to

deposit contacts [23].

$\text{Ga}_2\text{O}_3$  thin films in solar-blind UV photodetectors have been fabricated with several methods. A cation exchange mechanism was used to grow a bilayer of  $\text{Ga}_2\text{O}_3$  on  $\text{SnO}_2$  [24]. A photodetector with a  $\text{Ga}_2\text{O}_3$  thin film grown by laser molecular beam epitaxy has also been reported [25]. A  $\text{Ga}_2\text{O}_3$  UV photodetector was fabricated by evaporating gallium in oxygen plasma [26]. The floating zone method has also been used to fabricate  $\text{Ga}_2\text{O}_3$  for a UV photodetector [27]. Although many choices are available when fabricating  $\text{Ga}_2\text{O}_3$  thin films, most of these methods are expensive.

Solar blind photodetectors would be more commercially attractive if inexpensive methodologies of preparing  $\text{Ga}_2\text{O}_3$  are adopted. Emergent techniques of preparing monocrystalline  $\text{Ga}_2\text{O}_3$  films on top of GaN substrates using the floatation zone growth method hold great promise [28]. Alternatively, GaN thin films can be oxidized into  $\text{Ga}_2\text{O}_3$  at elevated temperatures prior to device fabrication [29].

In this work, we have developed a simple, rapid, and scalable method to convert the surface of (001)-oriented gallium arsenide (GaAs) wafers into macroporous  $\text{Ga}_2\text{O}_3$ . These films were then fabricated into highly sensitive  $\text{Ga}_2\text{O}_3$  photodetectors. The cost of GaAs wafers is roughly 10% that of GaN wafers. Additionally, it takes less than 1 hour to convert GaAs into  $\text{Ga}_2\text{O}_3$  using the approach outlined here, compared to hours for GaN. Given that the cost of GaN wafers is greater than 10 times that of GaAs, preparation of  $\text{Ga}_2\text{O}_3$  from GaAs is even more cost-effective than using thin film growth processes on GaN substrates. Using GaAs wafers as a source of  $\text{Ga}_2\text{O}_3$  is currently the least expensive and hence most economically viable method for mass manufacturing of solar blind photodetectors. In addition to being inexpensive, rapidly converting GaAs wafers into  $\text{Ga}_2\text{O}_3$  under high temperature results in a surface that is nanotextured. The fabricated devices therefore have higher sensitivity due to the increased sensing surface available for trapping incoming radiation [30]. Because the films are grown from the substrate, they are well-bonded, which gives the additional benefit of device robustness. The macro-porous surfaces of the grown film were continuous and provided large areas on which to deposit low-resistivity electrical contacts. Unlike with other approaches, the steps to grow these films are simple and inexpensive, suggesting that they can be further optimized to provide a viable solution to the aforementioned problems with current solar blind detectors.

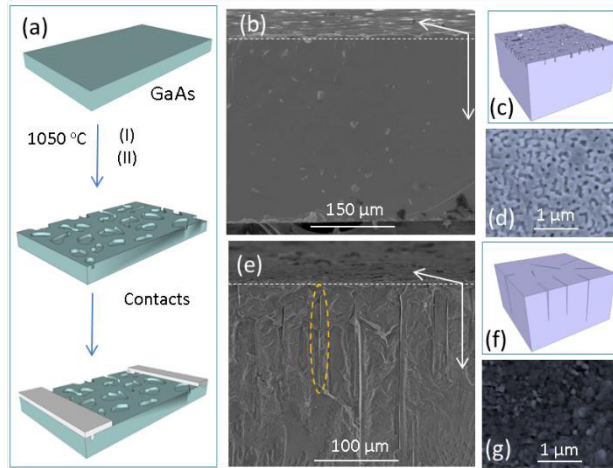


**Figure 1.** (a) Schematic of growth and fabrication process. The wafer is heated in the presence of (I) argon or (II) air followed by aluminum (Al) contact deposition with a separation of  $\sim 100\mu\text{m}$ . (b) A cross sectional SEM micrograph of  $\beta\text{-Ga}_2\text{O}_3$  prepared in argon gas. (c) A schematic view of the micrograph in (b) depicting the macro-porous nature of the surface. (d) A high magnification plan-view SEM micrograph showing the macro-pores on the surface of the wafer with a diameter of about 50 nm. (e) Another cross-sectional SEM micrograph of the  $\beta\text{-Ga}_2\text{O}_3$  prepared in the presence of air. Notice the long parallel micro-cracks that run perpendicular to the surface of the wafer indicated by the region highlighted in orange. (f) Another schematic view depicting the micro-cracks in the film grown in air. (g) A plan-view topographical SEM micrograph depicting stumps thought to be poorly nucleated  $\beta\text{-Ga}_2\text{O}_3$  with a nanowire-like structure.

## II. EXPERIMENTAL

As depicted in Fig. 1(a), a Si-doped GaAs wafer was placed into a horizontal quartz tube furnace and heated to 1050°C in an argon atmosphere for 40 minutes. Aluminum (Al) contact pads were then deposited on the processed wafer at a distance of  $\sim 100\mu\text{m}$ , as shown in the schematic. A cross-sectional scanning electron micrograph (SEM) of the  $\beta\text{-Ga}_2\text{O}_3$  (Ar) converted wafer and schematic of the surface are shown in Fig. 1(b) and 1(c) respectively. The porous surface structure is clearly visible in Fig. 1(b). Its plan-view SEM image (Fig. 1(d)) reveals a textured surface with irregular microgrooves and dimensions as small as 50 nm. For comparison, a similar wafer was heated in an oxygen rich atmosphere. A cross-sectional SEM image and schematic of its surface are shown in Figs. 1(e and f) which revealed narrow cracks running deep into the wafer. The plan-view SEM micrograph of the wafer prepared in air revealed the presence of poorly nucleated stumps, shown in Fig. 1(g).

For the samples synthesized in argon, it is thought that the oxygen originated from either the quartz tube or leakage into the chamber [31]. The growth process of the films can be explained using the well understood vapor–solid (VS) mechanism, given that no catalyst was used [32]. At the process temperature of 1050°C, the vapor pressure of arsenic is higher than that of gallium (Ga). This suggests that near the surface, the sample is slightly Ga-rich. According to the phase diagram, this induces a secondary phase of liquid Ga. It is thought that these gallium droplets slowly evaporate and react with oxygen at the GaAs solid surface.

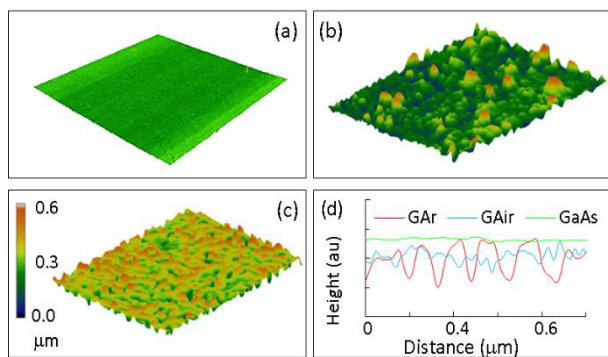


**Figure 2.** 3D micrographs of (a) GaAs, (b)  $\beta\text{-Ga}_2\text{O}_3$  grown in air ambient and (c)  $\beta\text{-Ga}_2\text{O}_3$  grown in argon atmosphere. These micrographs were generated from plan-view SEM images using Gwydion software. (d) Comparison of the surface roughness of the GaAs wafer,  $\beta\text{-Ga}_2\text{O}_3$  grown in air and  $\beta\text{-Ga}_2\text{O}_3$  grown in Ar as extracted from their respective micrographs.

SEM images of a pristine GaAs sample and samples that were thermally oxidized in air and argon atmospheres were transformed into 3-dimensional (3D) topographical micrographs, shown in Figs. 2(a-c), using Gwydion software to generate better comparative data of their surfaces. Akin to atomic force microscopy (AFM), the procedure allows for intuitive visualization [33]. The corresponding surfaces roughness values were extracted for each and correlated as depicted in Fig. 2(d). These extracted profiles make it easier to see the roughly 50 nm worm-like nanostructures on the surface of the sample processed in argon. It can be seen that the sample processed in oxygen has a more irregular surface structure with features sizes ranging from 10-150 nm.

## III. RESULTS AND DISCUSSION

X-ray diffraction (XRD) scans of both the sample processed in air and the sample processed in argon, acquired using Bragg-Brentano geometry, are shown in Fig. 3(a). Both air- and argon-prepared  $\text{Ga}_2\text{O}_3$  exhibited three strong peaks, (110), (-112), and (600) at  $31.74^\circ$ ,  $35.26^\circ$ , and  $38.42^\circ$   $2\theta$ , respectively. This diffraction pattern and the peak positions match well with the  $\beta\text{-Ga}_2\text{O}_3$  lattice constants of  $a = 12.23 \text{ \AA}$ ,  $b = 3.04 \text{ \AA}$ ,  $c = 5.80 \text{ \AA}$ , and  $\beta = 103.7^\circ$ , which confirms that the films were monoclinic. Energy-dispersive x-ray spectroscopy (EDX) was also conducted on the samples, as shown in Fig.

3(b). The spectrographs reveal a significant difference between the  $\beta$ -Ga<sub>2</sub>O<sub>3</sub> (air) and  $\beta$ -Ga<sub>2</sub>O<sub>3</sub> (Ar) samples. Whereas the spectrum from the sample grown in argon confirmed the presence of Ga and O in the predicted ratio of 2:3, it is evident that there were arsenic impurities in the sample prepared in air, as indicated by the additional peak at  $\sim 1.3$  keV. The presence of residual arsenic impurities on the  $\beta$ -Ga<sub>2</sub>O<sub>3</sub> sample prepared in air was confirmed by carrying out further EDX analysis of the cleaved wafer along its cross-section (not shown). It is hypothesized that arsenic did not fully evaporate from the GaAs oxidized in air given that its diffusion coefficient may be ambient dependent. Additionally, it is thought that the air stream into and out of the furnace reduced the temperature of the furnace and sample, resulting in remnants of arsenic after the reaction.

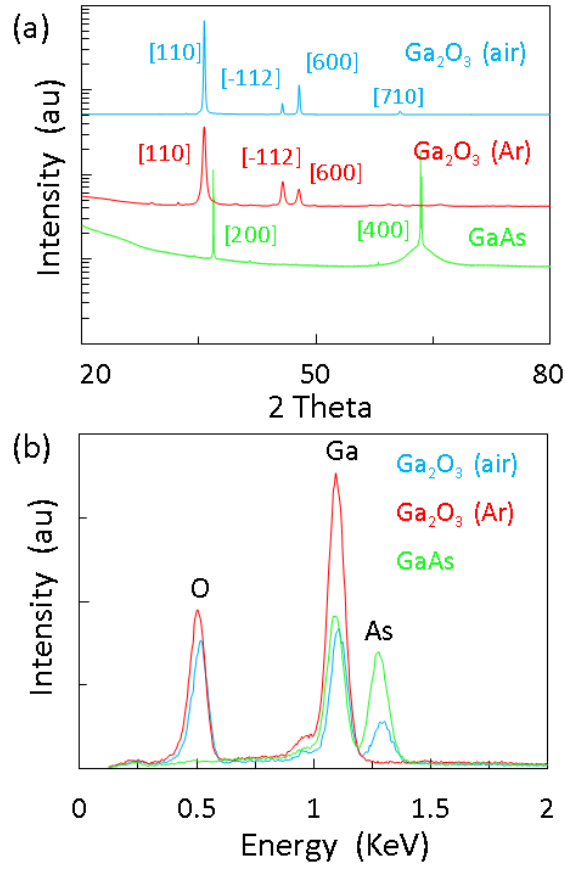


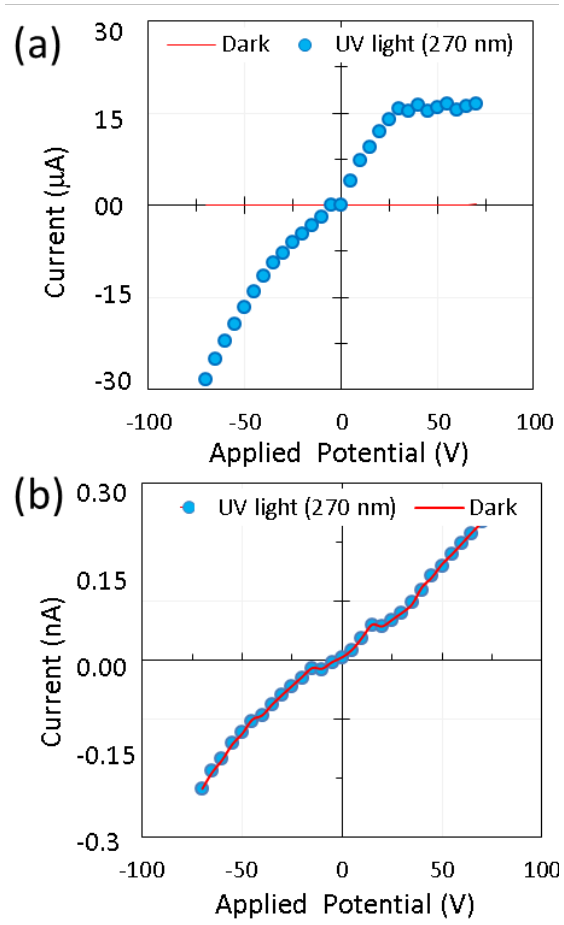
**Figure 3.** (a) XRD spectra of GaAs,  $\beta$ -Ga<sub>2</sub>O<sub>3</sub> prepared in air and  $\beta$ -Ga<sub>2</sub>O<sub>3</sub> prepared in argon. (b) EDX spectra of  $\beta$ -Ga<sub>2</sub>O<sub>3</sub> grown in air,  $\beta$ -Ga<sub>2</sub>O<sub>3</sub> grown in argon and the GaAs substrate. Note that the argon prepared  $\beta$ -Ga<sub>2</sub>O<sub>3</sub> has no detectable As peak, whereas the sample prepared in air has a strong presence of As.

$I$ - $V$  characteristics of the devices after contact deposition were measured in dark conditions and under UV illumination using a 270 nm source, shown in Fig. 4. The applied bias was varied from -80 to 80 V in steps of 5 V. The measurements were recorded at room temperature in ambient conditions. Under illumination, the sample prepared in argon exhibited a linearly increasing current as the applied bias was varied from 0 to 30 V. The current saturated above 30 V. The observed asymmetry of the ( $I$ - $V$ ) data is ascribed to the poor ohmic contacts between the contact pads and the device due to either the extremely low free carrier density within the  $\beta$ -Ga<sub>2</sub>O<sub>3</sub> or the mismatch of the work function between  $\beta$ -Ga<sub>2</sub>O<sub>3</sub> and Al contacts [34].

The photoconductive behavior is attributed to adsorption and desorption of oxygen molecules on the surface of  $\beta$ -

$\text{Ga}_2\text{O}_3$ , which typically hosts a high density of oxygen vacancies [35]. Under dark conditions, oxygen molecules may be adsorbed on the surface and trap free electrons, contributing to a depletion layer with reduced conductivity. Under optical illumination, electron-hole pairs are generated in  $\beta\text{-Ga}_2\text{O}_3$  and diffuse to the surface. Holes may then participate in the process of desorbing existing oxygen ions on the surface via the electron-hole recombination process. Electrons, on the other hand, would either be collected at the electrodes or recombine with holes that are generated when oxygen molecules are absorbed via an ionization process on the surface.

The measurements suggest that the device corresponding to the film grown in argon operated in the photoconductive mode. Its dark current was  $\sim 10$  nA while the ratio of the photocurrent generated under UV illumination to that of its dark current at 20 V was found to be  $1.6 \times 10^3$ . On the other hand, the  $\beta\text{-Ga}_2\text{O}_3$  grown in air did not exhibit distinctive solar-blind photodetector characteristics as shown in Fig. 4(b). It is speculated that arsenic within the sample, as confirmed by EDX, interfered with photocurrent generation. This may occur if arsenic species donate electrons during the oxygen adsorption step under dark conditions. This would effectively eliminate the depletion layer. Therefore, in the subsequent illumination step, even if excess holes are created in the bulk, there is no net concentration gradient to drive them toward the surface unlike in the pure  $\beta\text{-Ga}_2\text{O}_3$  case. The resulting  $I$ - $V$  data are therefore the same under dark and illuminated conditions.



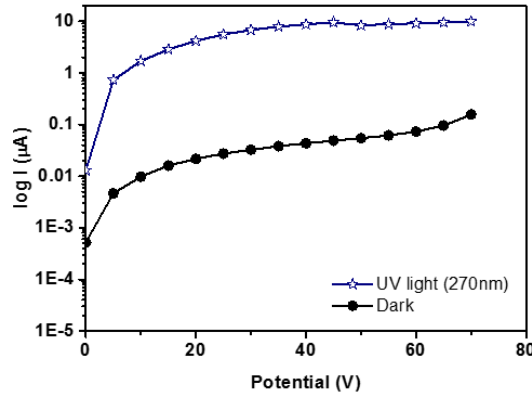


**Figure 4.** I-V characteristics of (a)  $\beta$ -Ga<sub>2</sub>O<sub>3</sub> (grown in an argon ambient) and (b)  $\beta$ -Ga<sub>2</sub>O<sub>3</sub> (grown in an air ambient), under dark and optical illumination with a 270 nm source. (c) is the graph in (a) plotted on a logarithmic scale. There is a three order increase in magnitude of the photocurrent in the argon prepared  $\beta$ -Ga<sub>2</sub>O<sub>3</sub> under a 270 nm UV light illumination while the  $\beta$ -Ga<sub>2</sub>O<sub>3</sub> sample prepared in air was non-responsive.

Fig. 5 (a) shows the time dependent photocurrent response of the  $\beta$ -Ga<sub>2</sub>O<sub>3</sub> (Ar) photodetector measured at applied biases of 5, 10 and 20 V. There is an increase in photocurrent with increasing bias: -5.10, 9.4, and 16.4  $\mu$ A at 5, 10, and 20 V, respectively. The higher biases help to separate photo-generated electron-holes pairs, resulting in higher photocurrents [36]. This behavior was highly reproducible over several hundred UV light on-off switches. The rise and decay times were also extracted from the photocurrent response. Here, rise time is defined as the time taken for the response current to increase from 10 % to 90 % of the maximum recorded current under illumination of UV light with a wavelength of 270 nm while the decay time is the time taken for the current to decrease from 90% to 10%. The measured rise times were 1.5 s at 5 V and 1.4 s at 10 and 20 V while the decay times were 0.5, 0.2, and 0.1 s at 5, 10, and 20V respectively. The rise time and decay times were found to decrease at 20 V compared to 5 and 10 V. The observed decreases in rise and decay time with increasing voltage are in agreement with the molecular sensitization and electron/hole trapping effect [37]. This hole-trapping mechanism through surface oxygen desorption in  $\beta$ -Ga<sub>2</sub>O<sub>3</sub> depends on applied voltage. In other words, a strong field caused by a higher bias voltage facilitates faster collection by the electrodes and inhibits the hole-trapping process. Thus, decreased rise and fall times are observed as the applied bias voltage is increased.

Fig. 5 (b) exhibits the effect of optical power on the photodetector response. The device exhibited a maximum current of 16.4  $\mu$ A at the highest incident optical power of 78  $\mu$ W/cm<sup>2</sup>. The device exhibited a linear increase in photocurrent with incident power. The spectral response is perhaps the most critical parameter for evaluating the device's potential as a solar blind photodetector. Fig. 5 (c) shows the responsivity of the  $\beta$ -Ga<sub>2</sub>O<sub>3</sub> (Ar) device measured from 200 to 400 nm. The device's maximum responsivity of 291.9 mA/W was observed at 270 nm under a bias of 20 V. This responsivity is much higher than that of AlGaIn-based photodetectors [38, 39] but less than photodetectors fabricated with MgZnO and Zr<sub>0.5</sub>Ti<sub>0.5</sub>O<sub>2</sub> [7], [40]. The corresponding calculated quantum efficiency was 1.34%.

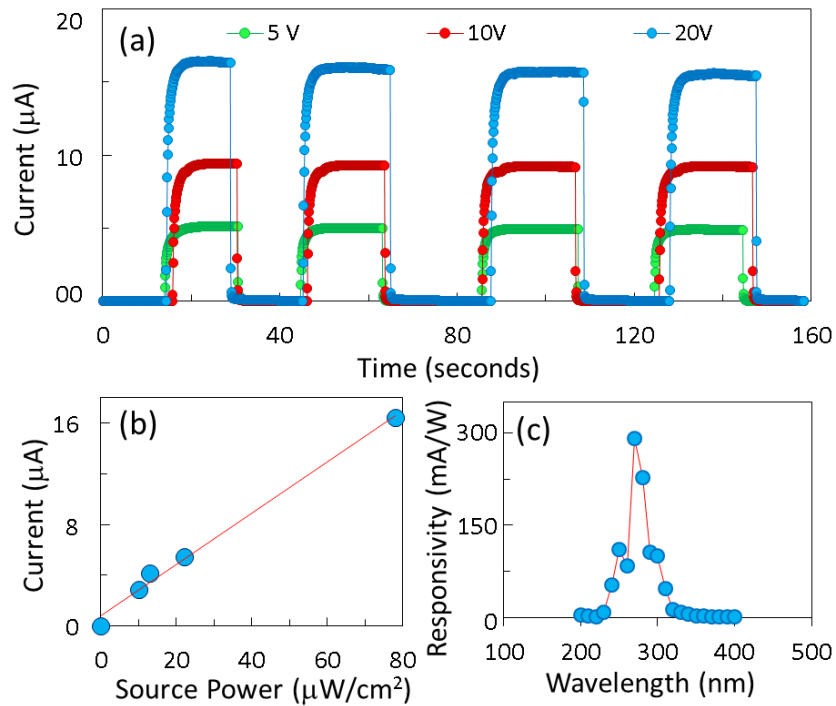


**Figure 5.** (a) Time response of  $\beta\text{-Ga}_2\text{O}_3$  (grown in Ar ambient) at 5, 10 and 20 V under alternating darkness and illumination at 270 nm wavelength. The detector has an extremely fast response and remains stable over many switching cycles (not shown). (b) The photo-response of argon prepare  $\beta\text{-Ga}_2\text{O}_3$  device with varied optical input power under 270 nm wavelength light at 20 V. Notice that there is linear correlation between the source power and the ensuing photocurrent. (c) Responsivity of the  $\beta\text{-Ga}_2\text{O}_3$  (grown in Ar ambient) device at 20V and 270 nm light illumination

#### IV. CONCLUSION

In summary, we have reported a simple growth and fabrication technique for solar-blind photodetectors that are sensitive to UV light. The nano-textured morphology of the  $\beta\text{-Ga}_2\text{O}_3$  surface grown from GaAs substrates under inert conditions acts as a photon trap for target illumination, thereby improving device sensitivity. The rugged device architecture provides for easier handling and removes pitfalls associated with contact formation of other devices derived from 1D nanostructures. Given that the starting materials are commercially available, this single step device fabrication scheme may be easily scaled to produce high yield, uniform solar blind photodetectors of high structural integrity.

**Acknowledgement:** The work reported herein was partially supported by an Army Research Office (ARO) research grant # W911NF-14-1-0341 and NSF grant # CMMI-1235592.

**Author information:** <sup>†</sup>Corresponding author email: sislam@ucdavis.edu

\*Dewyani Patil-Chaudhari<sup>1</sup>, Matthew Ombaba<sup>1</sup> contributed equally

#### REFERENCES

- [1] R. J. Zou, Z. Y. Zhang, J. Q. Hu, L. W. Sang, Y. Koide, and M. Y. Liao, "High-detectivity nanowire photodetectors governed by bulk photocurrent dynamics with thermally stable carbide contacts," *Nanotechnology*, vol. 24, Dec 2013.

- [2] P. Wang, Q. Zheng, Q. Tang, Y. Yang, L. Guo, F. Huang, *et al.*, "Dark current suppression of MgZnO metal-semiconductor-metal solar-blind ultraviolet photodetector by asymmetric electrode structures," *Optics Letters*, vol. 39, pp. 375-378, 2014/01/15 2014.
- [3] M. F. Anwar, A. Rivera, A. Mazady, H. C. Chou, J. W. Zeller, and A. K. Sood, "ZnMgO solar blind detectors: from material to systems," *Infrared Sensors, Devices, and Applications Iii*, vol. 8868, 2013 2013.
- [4] H. So, J. Lim, and D. G. Senesky, "Continuous V-Grooved AlGaIn/GaN Surfaces for High-Temperature Ultraviolet Photodetectors," *Ieee Sensors Journal*, vol. 16, pp. 3633-3639, May 15 2016.
- [5] L. Meiyong, S. Liwen, T. Teraji, M. Imura, J. Alvarez, and Y. Koide, "Comprehensive Investigation of Single Crystal Diamond Deep-Ultraviolet Detectors," *Japanese Journal of Applied Physics*, vol. 51, pp. 090115 (7 pp.)-090115 (7 pp.), Sept. 2012.
- [6] Y. H. Lai, Q. L. He, W. Y. Cheung, S. K. Lok, K. S. Wong, S. K. Ho, *et al.*, "Molecular beam epitaxy-grown wurtzite MgS thin films for solar-blind ultra-violet detection," *Applied Physics Letters*, vol. 102, pp. -, 2013.
- [7] M. Zhang, X. Gu, K. Lv, W. Dong, S. Ruan, Y. Chen, *et al.*, "High response solar-blind ultraviolet photodetector based on Zr<sub>0.5</sub>Ti<sub>0.5</sub>O<sub>2</sub> film," *Applied Surface Science*, vol. 268, pp. 312-316, Mar 1 2013.
- [8] M. Orita, H. Ohta, M. Hirano, and H. Hosono, "Deep-ultraviolet transparent conductive  $\beta$ -Ga<sub>2</sub>O<sub>3</sub> thin films," *Applied Physics Letters*, vol. 77, pp. 4166-4168, 2000.
- [9] X. Chen, K. W. Liu, Z. Z. Zhang, C. R. Wang, B. H. Li, H. F. Zhao, *et al.*, "Self-Powered Solar-Blind Photodetector with Fast Response Based on Au/ $\beta$ -Ga<sub>2</sub>O<sub>3</sub> Nanowires Array Film Schottky Junction," *Acs Applied Materials & Interfaces*, vol. 8, pp. 4185-4191, Feb 17 2016.
- [10] Y. Li, T. Tokizono, M. Liao, M. Zhong, Y. Koide, I. Yamada, *et al.*, "Efficient Assembly of Bridged  $\beta$ -Ga<sub>2</sub>O<sub>3</sub> Nanowires for Solar-Blind Photodetection," *Advanced Functional Materials*, vol. 20, pp. 3972-3978, 2010.
- [11] Q. N. Abdullah, F. K. Yam, K. H. Mohmood, Z. Hassan, M. A. Qaeed, M. Bououdina, *et al.*, "Free growth of one-dimensional  $\beta$ -Ga<sub>2</sub>O<sub>3</sub> nanostructures including nanowires, nanobelts and nanosheets using a thermal evaporation method," *Ceramics International*, vol. 42, pp. 13343-13349, Sep 2016.
- [12] Y. Bayam, V. J. Logeeswaran, A. M. Katzenmeyer, R. B. Sadeghian, R. J. Chacon, M. C. Wong, *et al.*, "Synthesis of Ga<sub>2</sub>O<sub>3</sub> Nanorods with Ultra-Sharp Tips for High-Performance Field Emission Devices," *Science of Advanced Materials*, vol. 7, pp. 211-218, Feb 2015.
- [13] Y. Kokubun, K. Miura, F. Endo, and S. Nakagomi, "Sol-gel prepared  $\beta$ -Ga<sub>2</sub>O<sub>3</sub> thin films for ultraviolet photodetectors," *Applied Physics Letters*, vol. 90, pp. -, 2007.
- [14] F. Boschi, M. Bosi, T. Berzina, E. Buffagni, C. Ferrari, and R. Fornari, "Hetero-epitaxy of epsilon-Ga<sub>2</sub>O<sub>3</sub> layers by MOCVD and ALD," *Journal of Crystal Growth*, vol. 443, pp. 25-30, Jun 1 2016.
- [15] N. M. Ghazali, M. R. Mahmood, K. Yasui, and A. M. Hashim, "Electrochemically deposited gallium oxide nanostructures on silicon substrates," *Nanoscale Research Letters*, vol. 9, Mar 17 2014.



- [16] S. Ghose, M. S. Rahman, J. S. Rojas-Ramirez, M. Caro, R. Droopad, A. Arias, *et al.*, "Structural and optical properties of beta-Ga<sub>2</sub>O<sub>3</sub> thin films grown by plasma-assisted molecular beam epitaxy," *Journal of Vacuum Science & Technology B*, vol. 34, Mar 2016.
- [17] Q. Feng, F. G. Li, B. Dai, Z. T. Jia, W. L. Xie, T. Xu, *et al.*, "The properties of gallium oxide thin film grown by pulsed laser deposition," *Applied Surface Science*, vol. 359, pp. 847-852, Dec 30 2015.
- [18] H. C. Kang, "Heteroepitaxial growth of multidomain Ga<sub>2</sub>O<sub>3</sub>/sapphire(001) thin films deposited using radio frequency magnetron sputtering," *Materials Letters*, vol. 119, pp. 123-126, Mar 15 2014.
- [19] W. Mi, J. Ma, C. N. Luan, and H. D. Xiao, "Structural and optical properties of beta-Ga<sub>2</sub>O<sub>3</sub> films deposited on MgAl<sub>2</sub>O<sub>4</sub> (100) substrates by metal-organic chemical vapor deposition," *Journal of Luminescence*, vol. 146, pp. 1-5, Feb 2014.
- [20] Y. Y. Lv, L. S. Yu, G. J. Zha, D. G. Zheng, and C. M. Jiang, "Application of soluble salt-assisted route to synthesis of beta-Ga<sub>2</sub>O<sub>3</sub> nanopowders," *Applied Physics a-Materials Science & Processing*, vol. 114, pp. 351-356, Feb 2014.
- [21] R. Korbutowicz, J. Prazmowska, Z. Wagrowski, A. Szyszka, and M. Tlaczala, "Wet thermal oxidation for GaAs, GaN and Metal/GaN device applications," *Asdam 2008, Conference Proceedings*, pp. 163-166, 2008.
- [22] W. S. Hwang, A. Verma, H. Peelaers, V. Protasenko, S. Rouvimov, H. Xing, *et al.*, "High-voltage field effect transistors with wide-bandgap beta-Ga<sub>2</sub>O<sub>3</sub> nanomembranes (vol 104, 203111, 2014)," *Applied Physics Letters*, vol. 104, Jun 16 2014.
- [23] N. Han, F. Wang, Z. Yang, S. Yip, G. Dong, H. Lin, *et al.*, "Low-temperature growth of highly crystalline beta-Ga<sub>2</sub>O<sub>3</sub> nanowires by solid-source chemical vapor deposition," *Nanoscale Research Letters*, vol. 9, Jul 10 2014.
- [24] W. E. Mahmoud, "Solar blind avalanche photodetector based on the cation exchange growth of beta-Ga<sub>2</sub>O<sub>3</sub>/SnO<sub>2</sub> bilayer heterostructure thin film," *Solar Energy Materials and Solar Cells*, vol. 152, pp. 65-72, Aug 2016.
- [25] X. C. Guo, N. H. Hao, D. Y. Guo, Z. P. Wu, Y. H. An, X. L. Chu, *et al.*, "beta-Ga<sub>2</sub>O<sub>3</sub>/p-Si heterojunction solar-blind ultraviolet photodetector with enhanced photoelectric responsivity," *Journal of Alloys and Compounds*, vol. 660, pp. 136-140, Mar 5 2016.
- [26] S. Nakagomi, T. Momo, S. Takahashi, and Y. Kokubun, "Deep ultraviolet photodiodes based on beta-Ga<sub>2</sub>O<sub>3</sub>/SiC heterojunction," *Applied Physics Letters*, vol. 103, Aug 12 2013.
- [27] R. Suzuki, S. Nakagomi, Y. Kokubun, N. Arai, and S. Ohira, "Enhancement of responsivity in solar-blind beta-Ga<sub>2</sub>O<sub>3</sub> photodiodes with a Au Schottky contact fabricated on single crystal substrates by annealing," *Applied Physics Letters*, vol. 94, Jun 1 2009.
- [28] R. Suzuki, S. Nakagomi, Y. Kokubun, N. Arai, and S. Ohira, "Enhancement of responsivity in solar-blind β-Ga<sub>2</sub>O<sub>3</sub> photodiodes with a Au Schottky contact fabricated on single crystal substrates by annealing," *Applied Physics Letters*, vol. 94, p. 222102, 2009.
- [29] T. J. H. W. Y. Weng, S. J. Chang, G. J. Huang and S. P. Chang, "A solar blind β gallium oxide nanowire photodetector," *IEEE Photonics Technology Letters*, vol. 22, pp. 709-711, 05/10/2010 2010.

- [30] M.-Y. Hwang, H. Kim, E.-S. Kim, J. Lee, and S.-M. Koo, "Enhanced photo-sensitivity through an increased light-trapping on Si by surface nano-structuring using MWCNT etch mask," *Nanoscale research letters*, vol. 6, pp. 1-8, 2011.
- [31] Y. Sakata, T. Nakagawa, Y. Nagamatsu, Y. Matsuda, R. Yasunaga, E. Nakao, *et al.*, "Photocatalytic properties of gallium oxides prepared by precipitation methods toward the overall splitting of H<sub>2</sub>O," *Journal of Catalysis*, vol. 310, pp. 45-50, Feb 2014.
- [32] X. Xiang, C. B. Cao, Y. Guo, and H. S. Zhu, "A simple method to synthesize gallium oxide nanosheets and nanobelts," *Chemical Physics Letters*, vol. 378, pp. 660-664, Sep 12 2003.
- [33] M. M. Ombaba, V. J. Logeeswaran, A. Ionescu, and M. S. Islam, "Integrating Ormosil films onto microstructured semiconductor substrates," *Acta Materialia*, vol. 72, pp. 159-166, Jun 15 2014.
- [34] J. Y. Z. P. Feng, Q. H. Li and T. H. Wang, "Individual  $\beta$  - Ga<sub>2</sub>O<sub>3</sub> nanowires as solar-blind photodetectors," *Applied Physics Letters*, vol. 88, pp. 153107-1-3, 2006.
- [35] L. Li, E. Auer, M. Y. Liao, X. S. Fang, T. Y. Zhai, U. K. Gautam, *et al.*, "Deep-ultraviolet solar-blind photoconductivity of individual gallium oxide nanobelts," *Nanoscale*, vol. 3, pp. 1120-1126, 2011.
- [36] Z. Zou, C. Xie, S. Zhang, C. Yang, G. Zhang, and L. Yang, "CdS/ZnO nanocomposite film and its enhanced photoelectric response to UV and visible lights at low bias," *Sensors and Actuators B-Chemical*, vol. 188, pp. 1158-1166, Nov 2013.
- [37] W. Y. Weng, T. J. Hsueh, S.-J. Chang, G. J. Huang, and S. C. Hung, "Growth of Ga<sub>2</sub>O<sub>3</sub> Nanowires and the Fabrication of Solar-Blind Photodetector," *Ieee Transactions on Nanotechnology*, vol. 10, pp. 1047-1052, Sep 2011.
- [38] L. van Schalkwyk, W. E. Meyer, F. D. Auret, J. M. Net, P. N. M. Ngoepe, and M. Diale, "Characterization of AlGa<sub>N</sub>-based metal-semiconductor solar-blind UV photodiodes with IrO<sub>2</sub> Schottky contacts," *Physica B-Condensed Matter*, vol. 407, pp. 1529-1532, May 15 2012.
- [39] E. Cicek, R. McClintock, Z. Vashaei, Y. Zhang, S. Gautier, C. Y. Cho, *et al.*, "Crack-free AlGa<sub>N</sub> for solar-blind focal plane arrays through reduced area epitaxy," *Applied Physics Letters*, vol. 102, pp. -, 2013.
- [40] Q. Zheng, F. Huang, K. Ding, J. Huang, D. Chen, Z. Zhan, *et al.*, "MgZnO-based metal-semiconductor-metal solar-blind photodetectors on ZnO substrates," *Applied Physics Letters*, vol. 98, pp. -, 2011.